DATA REPOSITORY ITEM 2012120

Melting under the Colorado Plateau, USA

Mary R. Reid

School of Earth Sciences and Environmental Sustainability, Northern Arizona University, Flagstaff, AZ 86011-4099, USA

Romain A. Bouchet, Janne Blichert-Toft

Université de Lyon, CNRS, UMR 5276, Laboratoire de Géologie de Lyon, Ecole Normale Supérieure de Lyon, 46 Allée d'Italie, 69364 Lyon Cedex 07, France

Alan Levander, Kaijian Liu

Department of Earth Science, Rice University, 6100 Main St., Houston, TX 77005, USA

Meghan S. Miller

Department of Earth Sciences, University of Southern California, Los Angeles, CA 90089,

USA

Frank C. Ramos

Department of Geological Sciences, New Mexico State University, Las Cruces, New Mexico, 88003, USA

Contents:

Item DR1. Supplementary seismological figures
Item DR2. Hafnium and Nd isotope data for Colorado Plateau-related volcanic rocks
Item DR3. Sources of major and trace element analyses of Colorado Plateau lavas
Item DR4. Background on Lu/Hf and Sm/Nd fractionation modeling, including effects of open system processes in the mantle source
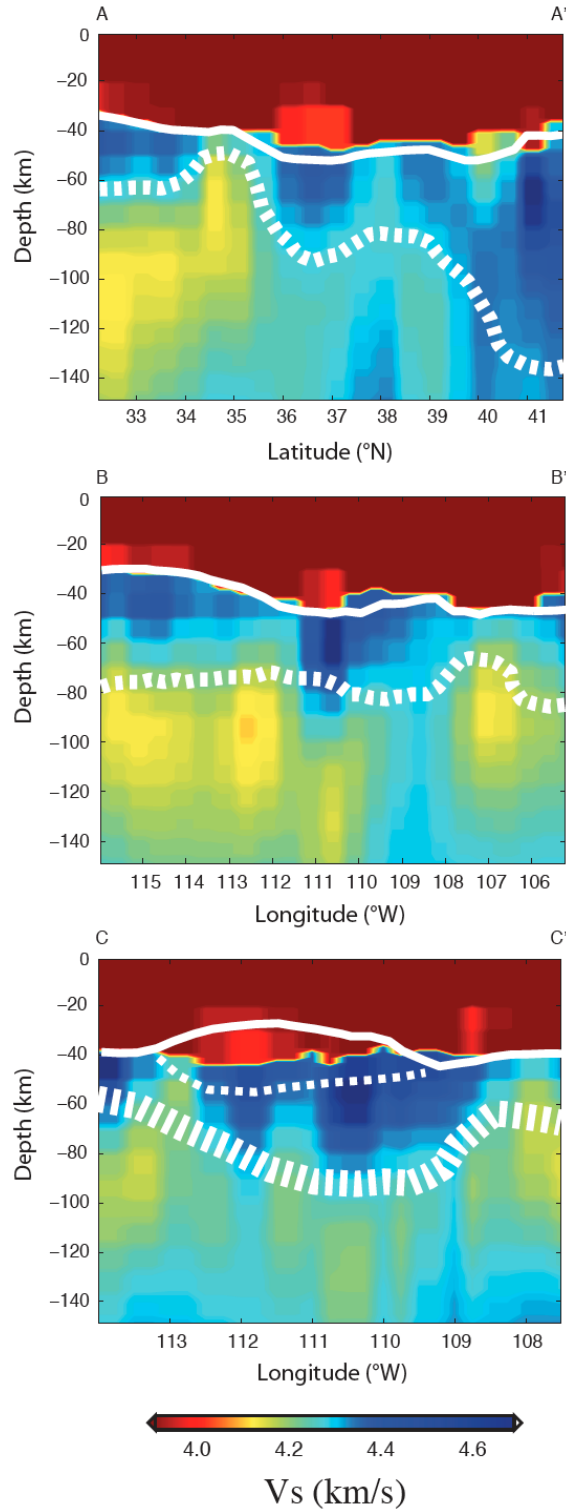
ITEM DR1. SUPPLEMENTARY SEISMOLOGICAL FIGURES

Figure DR1: Rayleigh wave V_s result (Liu et al., 2011) for cross-sections through the Colorado Plateau at locations shown in Figure 2 in paper; white lines as in that figure. The color scale represents the absolute value of V_s.
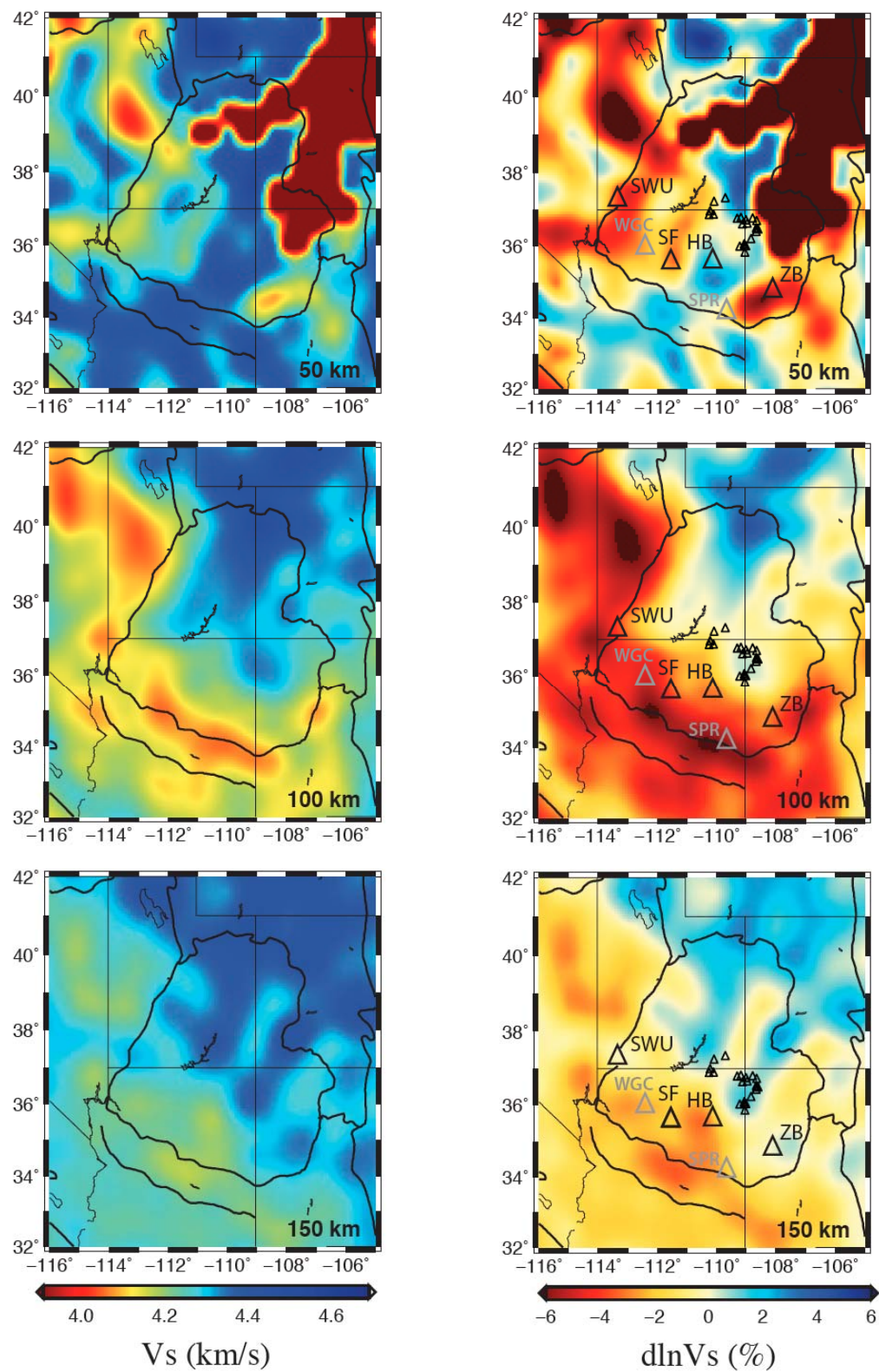
Figure DR2: Results of shear-wave tomography for 50 km depth intervals beneath the Colorado Plateau. Left hand figures show Vs; right hand figure shows dlnVs. Locations of volcanic fields shown in right hand figures.

ITEM DR2. SUMMARY OF Hf AND Nd ISOTOPE DATA FOR COLORADO PLATEAU LAVAS

Analytical Methods

Samples in addition to our own were obtained from Phil Kyle and Nelia Dunbar (Zuni Bandera Volcanic Field), Francis Albarède (Navajo Volcanic Field), David Moecher and Julie Floyd (San Francisco Volcanic Field), and Jim Hooten via Jorge Vazquez (Hopi Buttes). For those that were not already powdered, centimeter-sized samples were wrapped in plastic film and crushed using a hammer. Millimeter-sized pieces were then mixed to assure the homogeneity of the sampling, and powdered using an agate mortar and ethanol.

Hafnium and Nd isotopic compositions of powders were measured at the Ecole Normale Supérieure in Lyon using an integrated ion chromatographic separation protocol and MC-ICP-MS (a Nu Plasma HR). Hafnium and Nd isotopes were obtained from the same $HF-HNO_3$ sample attacks to eliminate artifacts from potential sample heterogeneity. For low-MgO samples (MgO < 10%), Hf was first leached out from the previously attacked samples using concentrated HF and then taken through a two-column purification scheme according to Blichert-Toft et al. (1997). The Ca-Mg fluoride precipitate left behind after the HF-Hf leaching procedure was redissolved in 2.5 M HCl and taken through a cation-exchange column to recover the REE-bearing fraction, which was then taken through an HDEHP column to separate Nd from the other REEs. For high-MgO samples (MgO > 10%), the HF leaching step was bypassed in order to maintain high Hf yields. Hafnium- and REE-containing fractions were instead separated on a cation-exchange column (Blichert-Toft, 2001) with subsequent Hf purification following the same column procedure as applied to the low-MgO samples, and Nd again separated from the other REEs on an HDEHP column (Blichert-Toft et al., 2005).

Both Hf and Nd were analyzed for their isotopic compositions on the Nu Plasma HR coupled with a desolvating DSN-100 nebulizer. Groups of two to four analyses of unknowns were bracketed by analyses of the JMC-475 Hf and "Rennes" in-house Nd (courtesy C. Chauvel) isotope standards and normalized for mass fractionation relative to, respectively, $^{179}Hf/^{177}Hf = 0.7325$ and $^{146}Nd/^{144}Nd = 0.7219$ using an exponential law. The JMC-475 Hf standard averaged 0.282160 ± 0.000010 (2s; n = 96) during the five Hf analytical sessions from June to November 2009, while the "Rennes" in-house Nd standard gave 0.511961 ± 0.000013 (2s; n = 40; see Chauvel and Blichert-Toft, 2001) during the three Nd analytical sessions between June and December 2010. The total procedural Hf and Nd blanks were less than 20 pg each.

Table DR1. Hf and Nd isotope data for Colorado Plateau volcanic rocks

Sample Number [a]	$^{176}Hf/^{177}Hf$ [b]	±2σ	$^{143}Nd/^{144}Nd$ [c]	±2σ	εHf [d]	εNd [d]	ΔεHf [d] (oceanic mantle)	ΔεHf [d] (terrestrial array)
San Francisco Volcanic Field								
R08SFVF01	0.282960	3	*0.51265*		6.65	0.23	3.14	3.33
SP Crater	0.282949	3	*0.51265*		6.26	0.23	2.75	2.94
R08SFVF03	0.282949	3	0.512756	5	6.25	2.30	-0.01	0.12
R08SFVF04	0.282971	3	*0.51288*		7.04	4.72	-2.44	-2.38
Merrium Cr. 2nd flow	0.282946	4	*0.51281*		6.17	3.36	-1.49	-1.40
R08SFVF05	0.282958	3	0.512674	6	6.58	0.70	2.44	2.62
Bonito	0.282962	3	*0.51275*		6.73	2.18	0.63	0.76
Marroon	0.282920	4	*0.51251*		5.23	-2.50	5.35	5.62
Strawberry	0.282948	4	*0.51264*		6.24	0.04	2.99	3.19
FR-SFVF2	0.282934	3	*0.51249*		5.73	-2.89	6.37	6.66
FR-SFVF3	0.282965	3	*0.51267*		6.83	0.62	2.80	2.98
FR-SFVF5	0.282965	5	*0.51260*		6.84	-0.74	4.62	4.84
FR-SFVF6	0.282994	3	*0.51278*		7.83	2.77	0.95	1.07
SC4	0.282970	4	0.512609	6	7.01	-0.56	4.55	4.77
SFVF003	0.282977	3	0.512687	6	7.25	0.95	2.79	2.96
SFVF004	0.283043	3	0.512774	6	9.59	2.65	2.87	2.99
SFVF05a	0.282974	3	0.512621	8	7.14	-0.34	4.39	4.60
SFVF05b	0.282970	3	0.512716	5	7.00	1.52	1.79	1.94
SFVF006	0.282969	4	0.512679	5	6.96	0.79	2.70	2.88
SFVF007	0.283053	3	0.512716	6	9.93	1.52	4.71	4.86
SFVF008	0.282975	3	0.512700	7	7.19	1.22	2.37	2.53
SFVF010	0.282938	4	0.512549	5	5.85	-1.73	4.95	5.20
SFVF011	0.282940	4	0.512552	5	5.95	-1.68	4.98	5.23
SFVF012	0.282938	3	0.512318	6	5.88	-6.24	10.98	11.37
SFVF013	0.282975	6	0.512561	10	7.19	-1.50	5.99	6.23
SFVF014	0.282919	4	0.512567	5	5.18	-1.39	3.84	4.08
SFVF016	0.282997	4	0.512692	9	7.96	1.05	3.37	3.54
SFVF017	0.282959	3	0.512607	4	6.62	-0.60	4.22	4.44
SFVF19a	0.282955	8			6.46			
SFVF19b	0.282976	10	0.512953	71	7.21	6.15	-4.17	-4.16
SFVF19c	0.282958	4	0.512760	5	6.57	2.37	0.22	0.35
SFVF19d	0.282952	3	0.512721	22	6.38	1.62	1.03	1.18
SFVF020	0.282950	4	0.512715	4	6.29	1.51	1.08	1.24
SFVF021	0.282981	5	0.512763	6	7.37	2.44	0.93	1.05
Zuni-Bandera Volcanic Field								
alkali basalts								
QB802	0.282989	4	0.512931	6	7.67	5.72	-3.13	-3.10
QBB301	0.282974	3	*0.512890*		7.14	4.92	-2.59	-2.54
QBB901a	0.282975	4	0.512892	5	7.18	4.96	-2.62	-2.57
QBO607	0.283016	3	0.512999	5	8.63	7.04	-3.93	-3.95
QBP601	0.282936	4	*0.512845*		5.80	4.04	-2.77	-2.69
QBP602	0.282920	3	*0.512841*		5.23	3.96	-3.23	-3.15
QV805	0.282971	3	*0.512901*		7.04	5.13	-2.99	-2.94
QVT301	0.282980	4	*0.512891*		7.36	4.94	-2.41	-2.36
tholeiitic basalts								
El Caulderon	0.282912	3	0.512761	5	4.94	2.40	-1.45	-1.32
North Plains	0.282854	4	0.512730	5	2.90	1.78	-2.67	-2.53

QB203	0.282899	4	*0.512913*		4.49	5.36	-5.84	-5.80
QBJ402	0.282896	4	0.512705	4	4.39	1.30	-0.54	-0.38
QBM502	0.282907	4	*0.512625*		4.77	-0.25	1.91	2.12
QBM801	0.282857	4	*0.512589*		3.02	-0.96	1.09	1.32
QBM803	0.282872	5	*0.512694*		3.54	1.09	-1.12	-0.95
QBT302	0.282904	4	*0.512701*		4.67	1.23	-0.17	0.00
QBW201	0.282932	4	*0.512711*		5.66	1.42	0.56	0.72
QBW203	0.282930	3	*0.512719*		5.59	1.58	0.29	0.44
QV101	0.282919	4	*0.512618*		5.20	-0.39	2.52	2.73
QV906	0.282929	4	0.512780	6	5.55	2.76	-1.32	-1.21
NM046	0.282942	4	0.512727	7	6.01	1.74	0.50	0.65
Southwestern Utah								
89UT01	0.282843	3	0.512432	6	2.50	-4.02	4.65	4.97
	0.282843	6			2.50		4.65	4.97
89UT02	0.282881	3	*0.51249*		3.86	-2.89	4.50	4.78
89UT03	0.282868	3	*0.51272*		3.38	1.60	-1.95	-1.79
	0.282870	3			3.46		-1.87	-1.72
89UT04	0.282808	4	0.512410	6	1.27	-4.45	3.99	4.33
	0.282814	1			1.47		4.19	4.52
89UT05	0.282664	3	*0.51212*		-3.82	-10.10	6.42	6.92
89UT06	0.282841	4	*0.51246*		2.43	-3.47	3.85	4.16
89UT07a	0.282817	3	*0.51230*		1.59	-6.59	7.16	7.55
89UT08	0.282811	5	*0.51233*		1.38	-6.01	6.17	6.55
89UT11	0.282746	3	*0.51232*		-0.92	-6.20	4.13	4.52
93UT15	0.282661	3	0.512238	7	-3.93	-7.80	3.25	3.68
			0.512225	7		-8.06	3.59	4.03
93UT16	0.282728	3	0.512221	6	-1.55	-8.13	6.07	6.51
Hopi Buttes								
ARJH10	0.282854	4	*0.512777*		2.90	2.71	-3.91	-3.79
OSJH2	0.282869	3	*0.512794*		3.43	3.04	-3.82	-3.71
FBJH3	0.282846	3	0.512793	5	2.62	3.01	-4.59	-4.48
ABJH2	0.282835	4	0.512785	8	2.23	2.87	-4.78	-4.67
Navajo Volcanic Field								
ShipRock	0.282803	3	0.512582	4	1.10	-1.10	-0.64	-0.41
Agathla	0.282852	3	0.512687	9	2.83	0.96	-1.65	-1.48
Cerros	0.282798	3	0.512667	4	0.92	0.56	-3.03	-2.85
Kayenta	0.282846	4	0.512650	4	2.62	0.23	-0.88	-0.69
NavajoWest	0.282812	3	0.512524	5	1.41	-2.22	1.16	1.43
NavajoEast	0.282816	4	0.512559	5	1.56	-1.54	0.40	0.65

[a] Sources for additional information on these samples are: Alibert et al. (1986); Menzies et al. (1991); Reid and Ramos (1996); Beard and Johnson (1997); Ramos (2000); Peters et al., 2008. Samples SFVF003-SFVF021 are from Dave Moecher and Julie Floyd, University of Kentucky. Other new samples here are: R08SFVF01 (SP Crater); R08SFVF02 (O'Neill Crater); R08SFVF04 (Sproul); R08SFVF05 (Kana-a flow, Sunset Crater).

[b] All Hf isotope data are new; values for two Navajo Volcanic Field samples are similar to those of Beard and Johnson (1997).

[c] New Nd isotope data shown in normal font. Data produced in other studies are shown in italics. Nd isotope data for SP Crater and Sproul from Ramos, 2000.

   (1) oceanic mantle array: $\Delta\varepsilon_{Hf} = \sum_{Hf} -(1.33 \cdot \sum_{Nd} + 3.2)$

   (2) terrestrial array: $\Delta\sum_{Hf} = \varepsilon_{Hf} -(1.36 \cdot \varepsilon_{Nd} + 3)$.

ITEM DR3. SOURCES OF MAJOR AND TRACE ELEMENT ANALYSES OF COLORADO PLATEAU LAVAS

Major and trace element and isotopic data for a variety of Colorado Plateau lavas are available through the Western North American Volcanic and Intrusive Rock Database (http://www.navdat.org). Additional analyses used for this study are those of Moore and Wolfe (1987), Newhall et al. (1987), Ulrich and Bailey (1987), Wolfe et al. (1987a, b), Arculus and Gust (1995), Hooten (1999), Ramos (2000), Peters et al. (2008), and new data presented in Table DR2.

Table DR2. Major and trace element analyses for lavas from southwestern Utah.
normalized to 100%

	89UT01	89UT02	89UT03	89UT04	89UT05	89UT06	89UT07	89UT08	89UT11	89UT15	89UT16
SiO_2	50.46	46.66	44.53	50.68	60.47	49.44	50.40	51.17	50.73	55.28	50.17
TiO_2	1.54	2.26	2.71	1.51	1.01	1.43	1.41	1.43	1.34	1.43	1.43
Al_2O_3	15.50	13.47	11.70	14.36	15.42	16.63	16.47	16.50	17.28	17.20	15.68
FeO_T	11.59	11.29	12.54	10.17	5.83	11.46	10.40	9.42	9.48	8.02	10.98
MnO										0.13	0.17
MgO	7.97	10.35	12.41	9.27	4.03	7.32	7.55	7.20	6.58	4.58	8.18
CaO	8.91	10.74	10.92	9.31	5.61	9.82	9.54	9.49	10.08	6.94	9.09
Na_2O	3.14	3.17	2.98	3.19	4.45	3.28	3.34	3.45	3.37	3.83	3.10
K_2O	0.65	1.41	1.42	1.10	2.65	0.43	0.74	1.01	0.84	2.12	0.95
P_2O_5	0.23	0.66	0.79	0.40	0.54	0.18	0.16	0.32	0.30	0.49	0.26

ITEM DR4. BACKGROUND ON Lu/Hf AND Sm/Nd FRACTIONATION MODELING, INCLUDING EFFECTS OF OPEN SYSTEM PROCESSES IN THE MANTLE SOURCE

DR4.1 Significance of Lu/Hf and Sm/Nd Fractionation Factors (α_{Hf} and α_{Nd}, respectively)

Garnet can significantly fractionate the rare earth elements from each other and also from Hf. Lithosphere of the thickness of the Colorado Plateau (CP) spans depths where garnet should be stable to depths where garnet should be absent in normal mantle peridotite (z>75 km). Thus, the magnitudes of Sm-Nd and Lu-Hf fractionation are expected to vary with melting depth. Reference curves for the effects of melting in the presence of garnet peridotite and spinel peridotite on derivative magmas are shown in Figure 4 in paper and Figure DR3. The alpha values represent the fractionation of the parent and daughter elements associated with the Lu-Hf and Sm-Nd decay schemes, respectively, i.e.,

$$\alpha_{Hf} = [F + D_{Hf}(1\text{-}F)/[F + D_{Lu}(1\text{-}F)], \ \ \alpha_{Nd} = [F + D_{Nd}(1\text{-}F)/[F + D_{Sm}(1\text{-}F)].$$

Comparison of these two curves shows that the fractionation of Lu-Hf is strongly controlled by the presence or absence of garnet whereas Sm-Nd fractionation is more strongly influenced by the degree of partial melting. If, for example, CP melts were produced entirely in the stability field of spinel peridotite, the magnitude of trace element fractionation should lie along the curve for spinel peridotite, with their specific positions dictated by the extent of partial melting responsible for the melts.

The data presented here and previously (Alibert et al., 1986; Beard and Johnson, 1997) show that CP melts are being generated in reservoirs that are isotopically distinct from those that typify the asthenospheric upper mantle and, at least generally, also distinct from deeper-seated sources such as those responsible for ocean island basalts. Melting of the lithosphere may be responsible for the mafic CP lavas, an interpretation that is also in keeping with the pressures estimated for melt equilibration (Lee et al., 2009). Accordingly, the lavas may sample mantle domains that have been isolated from the convecting upper mantle since crustal stabilization 1.74 to 1.6 b.y. ago (Bennett and DePaolo, 1987). Combining this estimate for the storage time of the mantle lithosphere with the Hf and Nd isotope compositions measured in the lavas enables us to estimate time-integrated Lu/Hf and Sm/Nd ratios for the magma sources. The ratio between measured and time-integrated parent-daughter ratios is a potential measure of melting-induced trace element fractionation and can also be expressed using the alpha notation as follows:

$$\alpha_{Hf} = (\text{Lu/Hf})_{measured}/(\text{Lu/Hf})_{time\text{-}integrated}$$

and

$$\alpha_{Nd} = (\text{Sm/Nd})_{measured}/(\text{Sm/Nd})_{time\text{-}integrated} \ .$$

Figure 4 in the paper shows how the fractionation factors for CP lavas compare to those expected for melting in the presence of spinel and garnet peridotite. Time-integrated

Lu/Hf and Sm/Nd are estimated from the present-day ^{176}Hf/^{177}Hf and ^{143}Nd/^{144}Nd composition of the lavas, assuming initial ratios (0.281890 and 0.510603, respectively) that correspond to Paleoproterozoic depleted mantle at 1.75 Ga (ε_{Hf} = +8 and ε_{Nd} = +4.5). Based on the overall trend exhibited by the chemical and isotopic characteristics of the lavas, the more extreme Lu-Hf and Sm-Nd fractionations can be explained by small degrees of melting in the presence of garnet whereas less pronounced fractionations require contributions from larger degree melts from other sources.

DR4.2. Effect of Recent Open-System Modification of the Mantle on α_{Hf} - α_{Nd} Interpretations

Recent workers have suggested that mantle under areas of CP volcanism has been modified by intrusions of asthenosphere-derived magmas with depleted mantle isotopic and chemical signatures. To demonstrate how recent open-system behavior of the mantle might influence the results presented in Fig. 4 in the paper, trends defined by subtracting the chemical and isotopic signatures of asthenospheric melts and their mineral precipitates from intermediate and high α_{Hf}- α_{Nd} value melts were determined. Unmixing trends for three erupted lavas are shown in Figure DR3. The alpha-alpha characteristics are calculated from the resulting ^{147}Sm/^{144}Nd, ^{176}Lu/^{177}Hf, and isotopic compositions as models for the mantle prior to modification. Calculated trends assume that the invasive melts are alkaline melts of depleted mantle such as those erupted at Zuni-Bandera, New Mexico. Comparable melts from Lunar Crater, Nevada, and Cima, California, yield similar effects. Numbers adjacent to the tic points or at the ends of the curves indicate the fraction of asthenospheric component subtracted (F_{asth}). In most cases, they are maximum values delimited by departures of the unmixing arrays from conditions permitted by spinel peridotite, garnet peridotite, eclogite, and garnet pyroxenite melting. Maximum F_{asth} for many is <15%.

Even though simplified, the unmixing curves in the Figure DR3 models provide insight into the possible range of open system effects. Curves with dual tic marks in Figure DR3 (solid orange lines) show how inferences about the conditions of mantle melting would change if the possible effects of hybridization of ambient mantle or its melts with bulk asthenospheric melts are subtracted. These trends were obtained by subtracting the isotopic and trace element influences of alkaline asthenospheric melts from the erupted melt (reversing the possible effects of mixing between melts of the asthenosphere and lithosphere) or from an ambient mantle responsible for the CP melts (reversing the effect of cryptic metasomatism of enriched lithospheric mantle by small degree melts of the asthenosphere). For the latter, melt derivation by 3-20% partial melting is assumed, as estimated from α_{Nd} for individual lavas (see Figure 4 in paper). Partition coefficients for estimating the chemistry of the ambient mantle source from lava composition are D_{Sm} = 0.045, D_{Nd} = 0.023, D_{Lu} = 0.073, and D_{Hf} = 0.035, assuming a source with 85% olivine + orthopyroxene, 12% clinopyroxene, and 3% spinel (partition coefficient data of Salters and Longhi, 1999). In detail, the partial melt fraction and specific partition coefficients depend on the extent of mantle metasomatism but this is a negligible source of uncertainty for the inferences presented here. As can be anticipated from the trend defined by the α_{Hf} - α_{Nd} values of the lavas overall, if the chemical and isotopic compositions of the CP lavas reflect mixtures of melts from depleted and enriched mantle sources, then an enriched ambient mantle with higher α_{Hf} and α_{Nd} than the

lavas is required. Accordingly, partial melting at even shallower conditions would be required to explain the paired chemical and isotopic characteristics of the enriched end member. The resulting "unmixing" trends for the two cases are essentially identical except that potential contributions from depleted mantle melts are permitted to be larger in the case of magma mixing.

An alternate scenario to hybridization involving bulk asthenospheric melts is modal metasomatism by minerals precipitated as such melts ascend, cool, and crystallize. Common minerals deposited by mafic melts that could significantly alter Sm/Nd and Lu/Hf ratios are clinopyroxene and garnet. Three sets of curves in Figure DR3 show how the α_{Hf} - α_{Nd} characteristics for ambient mantle melting would differ if the observed melt chemistry is influenced by these metasomatic assemblages. CP melts are again assumed to represent 3-20% partial melting of the metasomatized mantle and curves show how inferences about the conditions and degree of partial melting would change if the effects of metasomatic minerals were isolated from that of the ambient mantle.

If the melt characteristics of the CP lavas are influenced by garnets precipitated from alkaline depleted mantle melts, then melts of the ambient mantle are predicted to have been similar in their Sm/Nd but higher in Lu/Hf, and therefore require melting at lower pressures. Removing the possible control of a clinopyroxenite metasomatic assemblage predicts bulk melt generation by larger degree melting at lower pressure.
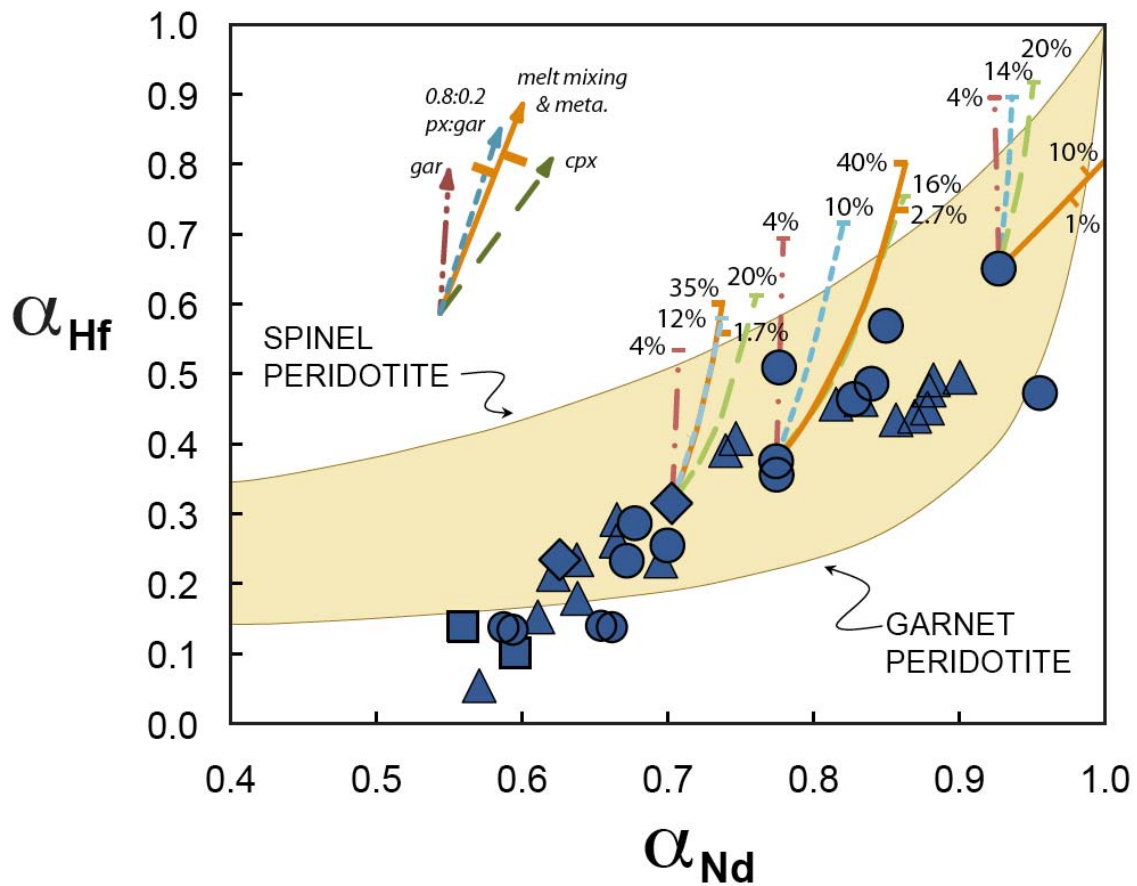
Figure DR3: Plot showing how melting conditions inferred for Colorado Plateau lavas from their α_{Hf} and α_{Nd} characteristics would change if their sources are influenced by contributions from depleted asthenospheric melts and their minerals. Curves are for mixing between depleted asthenospheric mantle melts and enriched "lithospheric" melts or mantle (orange solid lines), metasomatism by addition of clinopyroxene (green long dash line), garnet (red dash-dot lines), and clinopyroxene and garnet in 4:1 proportions (turquoise short dash lines). Numbers indicate the amount of depleted mantle melts or minerals removed at the α_{Hf} - α_{Nd} values of the associated tic mark. "Unmixing" trends involving bulk depleted mantle melts (orange solid lines) are identical except that potential contributions from depleted mantle melts are permitted to be larger in the case of magma mixing (left tic marks) than cryptic metasomatism (right tic marks). Field shows range of α_{Hf} - α_{Nd} values permitted by melting of spinel and garnet peridotite, eclogite, and garnet pyroxenite melting. See text above for details.

References Cited

Alibert, C., Michard, A., and Albarede, F., 1986, Isotope and trace element geochemistry of Colorado Plateau volcanics: Geochimica et Cosmochimica Acta, v. 50, p. 2735–2750.

Arculus, R.J. and Gust, D.A., 1995, Regional petrology of the San Francisco Volcanic Field, Arizona, USA: Journal of Petrology, v. 36, p. 827-861.

Beard, B.L., Johnson, C.M., 1997, Hafnium isotope evidence for the origin of Cenozoic basaltic lavas from the southwestern United States: Journal of Geophysical Research 102, 20149–20178.

Bennett, V.C., and DePaolo, D.J., 1987, Proterozoic crustal history of the western United States as determined by neodymium isotopic mapping: Geological Society of America Bulletin, v. 99, p. 674–685.

Blichert-Toft, J. and Albarède, F., 1997, The Lu-Hf isotope geochemistry of chondrites and the evolution of the mantle-crust system. Earth and Planetary Science Letters, v. 148, p. 243-258.

Blichert-Toft, J., Chauvel, C., and Albarède, F., 1997, Separation of Hf and Lu for high-precision isotope analysis of rock samples by magnetic sector-multiple collector ICP-MS: Contributions to Mineralogy and Petrology, v. 127, p. 248-260.

Blichert-Toft, J., 2001, On the Lu-Hf isotope geochemistry of silicate rocks: Geostandards Newsletter, v. 25, p. 41-56.

Blichert-Toft, J., Agranier, A., Andres, M., Kingsley, R., Schilling, J.-G., and Albarède, F., 2005. Geochemical segmentation of the Mid-Atlantic Ridge north of Iceland and ridge-hot spot interaction in the North Atlantic: Geochemistry, Geophysics, Geosystems, v. 6, Q01E19, doi:10.1029/2004GC000788.

Chauvel, C. and Blichert-Toft, J., 2001, A hafnium isotope and trace element perspective on melting of the depleted mantle: Earth and Planetary Science Letters, v. 190, p. 137-151.

Crowley, J.L., Schmitz, M.D., Bowring, S.A., Williams, M.L., and Karlstrom, K.E., 2006, U–Pb and Hf isotopic analysis of zircon in lower crustal xenoliths from the Navajo volcanic field: 1.4 Ga mafic magmatism and metamorphism beneath the Colorado Plateau: Contributions to Mineralogy and Petrology, v. 151, p. 313–330, doi: 10.1007/s00410-006-0061-z.

Hooten, J.A., 1999, Phreatomagmatic Diatremes of the Western Hopi Buttes Volcanic Field, Nation, Arizona, M.S. Thesis, Northern Arizona University, 140p.

Johnson, C.M. and B.L. Beard, B.L., 1993, Evidence from hafnium isotopes for ancient sub-oceanic mantle beneath the Rio Grande rift region, S.W.U.S.A.: Nature, v. 362, p. 441-444.

Lee, C.-T., Luffi, P., Plank, T., Dalton, H., and Leeman, W.P., 2009, Constraints on the depths and temperatures of basaltic magma generation on Earth and other terrestrial planets using new thermobarometers for mafic magmas: Earth and Planetary Science Letters, v. 279, p. 20–33

Liu, K., Levander, A., Niu, F., and Miller, M.S., 2011, Imaging crustal and upper mantle structure beneath the Colorado Plateau using finite-frequency Rayleigh wave tomography: Geochemistry, Geophysics, Geosystems, 12, Q07001, doi:10.1029/2011GC003611.

Menzies, M.A., Kyle, P.R., Jones, M., and Ingram, G., 1991, Enriched and depleted source

components for tholeiitic and alkaline lavas from Zuni-Bandera, New Mexico: Inferences about intraplate processes and stratified lithosphere: Journal of Geophysical Research, v. 96, p. 13645-13672.

Moore, R.B. and Wolfe, E.W., 1987, Geologic map of the east part of the San Francisco volcanic field, north-central Arizona: U.S. Geological Survey Miscellaneous Field Studies Map MF-1960, scale 1:50 000.

Newhall, C.G., Ulrich, G.E., and Wolfe, E.W., 1987, Geologic map of the southwest part of the San Francisco volcanic field, north-central Arizona: U.S. Geological Survey Miscellaneous Field Studies Map MF-1958, scale 1:50 000.

Peters, T.J., Menzies, M., Thirlwall, M., and Kyle, P.R., 2008, Zuni–Bandera volcanism, Rio Grande, USA — Melt formation in garnet- and spinel-facies mantle straddling the asthenosphere–lithosphere boundary: Lithos, v. 102, p. 295-315.

Ramos, F. C., 2000, Mantle sources generating recent volcanism in the Western US: Ph.D. thesis, University of California, Los Angeles.

Reid, M.R. and Ramos, F.C., 1996, Chemical dynamics of enriched mantle in the southwestern United States: thorium isotope evidence: Earth and Planetary Science Letters, v. 138, p. 67-81.

Salters, V. J. M. and Longhi, J. E., 1999, Trace element partitioning during the initial stages of melting beneath ocean ridges: Earth and Planetary Science Letters, v. 166, p. 15–30.

Ulrich, G. E., and Bailey, N. G., 1987, Geologic map of the SP Mountain part of the San Francisco volcanic field, north-central Arizona: U.S. Geological Survey Miscellaneous Field Studies Map MF-1956, scale 1:50 000.

Vervoort, J.D., Patchett, P.J., Blichert-Toft, J., and Albarède, F., 1999, Relationships between Lu-Hf and Sm-Nd isotopic systems in the global sedimentary system: Earth and Planetary Science Letters, v. 168, p. 79-99.

Wolfe, E. W., Ulrich, G. E., Holm, R. F., Moore, R. B., and Newhall, C. G., 1987a, Geologic map of the central part of the San Francisco volcanic field, north-central Arizona: U.S. Geological Survey Miscellaneous Field Studies Map MF-1959, scale 1:50 000.

Wolfe, E.W., Ulrich, G.E., and Newhall, C.G., 1987b, Geologic map of the northwest part of the San Francisco volcanic field, north-central Arizona: U.S. Geological Survey Miscellaneous Field Studies Map MF-1957, scale 1:50 000.